33rd Annual International Conference of the IEEE EMBS
Boston, Massachusetts USA, August 30 - September 3, 2011

An ICA-Based Method for the Segmentation of Pigmented Skin Lesions in Macroscopic Images

Pablo G. Cavalcanti, Jacob Scharcanski, Leandro E. Di Persia and Diego H. Milone

Abstract— **Segmentation is an important step in computer-aided diagnostic systems for pigmented skin lesions, since that a good definition of the lesion area and its boundary at the image is very important to distinguish benign from malignant cases. In this paper a new skin lesion segmentation method is proposed. This method uses Independent Component Analysis to locate skin lesions in the image, and this location information is further refined by a Level-set segmentation method. Our method was evaluated in 141 images and achieved an average segmentation error of 16.55%, lower than the results for comparable state-of-the-art methods proposed in literature.**

I. INTRODUCTION

Pigmented skin lesions include both, benign and malignant forms. Just in United States of America occur about 10000 deaths per year from the 40000 to 50000 diagnosed cases of melanoma, a dangerous kind of malignant pigmented skin lesions. Early diagnosis is of fundamental importance to improve the patient prognosis, nevertheless discriminating benign from malignant skin lesions has been proven to be a challenging task.

To facilitate the diagnosis, physicians often use dermoscopy, which is a non-invasive technique that magnifies submacroscopic structures with the help of an optical lens (a dermoscope) and liquid immersion. According to Mayer [1], the use of dermoscopy can increase the diagnosis sensitivity in 10-27% with respect to the clinical diagnosis. The early diagnosis of melanomas is very important for the patient prognosis, since most malignant skin lesion cases can be treated successfully in their early stages. However, even with the help of dermoscopy, differentiating malignant and benign lesions is a hard task. In fact, specialists affirm that in the early stages of the evolution of malignant lesions, dermoscopy may be useless as a tool to help the diagnosis [2].

Still considering early stage cases, there are practical situations where a non-specialist (e.g. a physician not trained on Dermatology) wishes to have a qualified opinion about a suspect skin lesion, but only standard camera imaging is available on site. In such situations, telemedicine is justifiable, and the non-specialist can capture an image of the suspect skin lesion and send it to an specialist, who can analyze it in higher detail. In this particular situation, a teledermatology consultation brings benefits, like the easier access to health care and faster clinical results [3]. Besides, comparing the physical (face-to-face) patient diagnosis with the remote diagnosis by teledermatology, recent results suggest that teledermatology also tends to be effective and reliable [4]. Therefore, there is a growing interest in methods for diagnosing pigmented skin lesions remotely, and segmentation is important in this context since the lesion must be correctly located before it is analyzed and diagnosed.

Many segmentation methods have been proposed in the literature for dermoscopy images. Such techniques often are based on different strategies, namely: region-based, using mainly region-growing approaches [5] [6]; clustering algorithms, separating healthy and unhealthy pixels in homogeneous regions [7]; thresholding methods, computing values that can identify the lesion in histograms [8]; and, active contours procedures, where the lesion borders are detected iteratively [9]. In a literature review, Celebi et al. [10] reported that most of these methods are automatic and operate on color images, but usually can result on segmentation errors, specially closer to the lesion borders.

Unfortunately, macroscopic pigmented skin lesion (MPSL) image segmentation did not receive much attention in the literature. Recently, some experiments [11] [12] demonstrated that active contours-based techniques can achieve good results. However, these methods usually depend on good initialization, and in our case this is not easily attainable. MPSL images usually contain several artifacts (as uneven illumination condition, hair, freckles, etc.) that make the automatic segmentation of the lesion region more difficult, and manual initialization often becomes necessary. In this paper, we propose a method based on Independent Component Analysis (ICA), that detects the skin lesion in macroscopic images, and uses this approximation as an initialization of a Level-set method that detects the lesion boundaries more accurately.

In Section II we describe all the steps of this method. Then, in Section III we present our segmentation results for publicly available datasets. Finally, Section IV presents conclusions and directions for future work.

II. PROPOSED METHOD FOR SKIN LESION SEGMENTATION

As mentioned before, MPSL images usually contain artifacts that make the automatic lesion segmentation more difficult. Shading is a particularly challenging artifact, since shading areas often are darker than healthy skin and may be confused with lesion areas. To avoid confusing lesion and shading areas, the first step of our segmentation method is

Pablo G. Cavalcanti and Jacob Scharcanski are with the Instituto de Informática, Universidade Federal do Rio Grande do Sul. Avenida Bento Gonçalves, RS, Brazil 91501-970 {pgcavalcanti,jacobs}@inf.ufrgs.br.

Leandro E. Di Persia and Diego H. Milone are with Facultad de Ingeniera y Ciencias Hdricas, Universidad Nacional del Litoral, Paraje El Pozo, Santa Fe, Argentina, S3000, and the National Council for Science and Technology (CONICET) {ldipersia,dmilone}@fich.unl.edu.ar

to attenuate the local shading effects. After that, we use ICA to separate the information contained in the image, usually healthy skin, lesion and possibly other artifacts. Given the ICA results we obtain an initial lesion localization, and then the lesion boundary is determined more accurately by using a Level-set method [13] and a few post-processing steps. All these steps are detailed in the following subsections.

A. Shading Attenuation

Cavalcanti et al. [14] [15] recently proposed a method to significantly attenuate shading effects in MPSL images. The method assumes that images are acquired in a way that the lesion appears in the image center, and it does not touch the image outer borders. The first step of the method is to convert the image from the original RGB color space to the HSV color space, and retain the Value channel V. This is justified by the fact that this channel presents the higher visibility of the shading effects. We extract 20×20 pixels in each V corner and define S as the union of these four sets. This pixel set is used to adjust the following quadric function $z(x, y)$:

$$z(x, y) = P_1 x^2 + P_2 y^2 + P_3 xy + P_4 x + P_5 y + P_6, \quad (1)$$

where the six quadric function parameters P_i $(i = 1, ..., 6)$ are chosen to minimize the error ϵ:

$$\epsilon = \sum_{j=1}^{N_s} \left[V(S_{j,x}, S_{j,y}) - z(S_{j,x}, S_{j,y}) \right]^2, \quad (2)$$

where, $S_{j,x}$ and $S_{j,y}$ are the x and y coordinates of the jth element of the set S, respectively, and N_s is the total number of pixels of the four corners ($N_s = 1600$ in our experiments).

Calculating the quadric function $z(x, y)$ for each image spatial location (x, y), we have an estimate $z(x, y)$ of the local illumination intensity in the image $V(x, y)$. Dividing the original $V(x, y)$ channel by $z(x, y)$, we obtain a new Value channel where the shading effects have been attenuated. The final step is to replace the original Value channel by this new Value channel, and convert the image from the HSV color space to the original RGB color space.

B. ICA-Based Lesion Localization

Independent Component Analysis (ICA) is a method to process multivariate data, producing projections that are as statistical independent as possible [16]. In this way, ICA searches for a data projections that maximize the degree of independence of such data projection. In this work, we use the FastICA algorithm [17] with a cost function that maximizes non-Gaussianity. To apply FastICA, we resize each $n \times m$ image channel to a $1 \times nm$ vector, by scanning the image top to bottom, left to right, and normalize color image triplet components to unity length [1], obtaining the $3 \times nm$ measure matrix X. Then, the FastICA algorithm searches for a separation matrix W such that the output matrix $Y = WX$ has row components that are as statistically independent as possible.

[1]The ICA assumes that samples are iid, and scanning order is irrelevant.

Applying the ICA to MPSL images three independent components are obtained, one corresponds mainly to the lesion area, another to the healthy skin, and the third component corresponds to noise and other artifacts. Nevertheless, there is an ordering indeterminacy inherent to the ICA method, and it is not possible to know in advance which component will show the lesion more clearly. However, due to the lesion variability, the histogram of the component that shows more clearly the lesion often has a non-Gaussian histogram (frequently multimodal). The histogram of the component showing predominantly noise and artifacts tends to be non-Gaussian, and the component that shows healthy skin more clearly tends to have a Gaussian histogram. Thus, we measure the non-Gaussianity of the ICA histogram components with differential entropy, i.e. $\mathcal{J}(\mathcal{X}) = |H(\mathcal{X}) - H(\mathcal{X}_g)|$, where $\mathcal{X}_g$ is a Gaussian distributed random variable with the same variance as $\mathcal{X}$. The component that produces the largest differential entropy is identified as the one containing the lesion information more clearly, and the smallest differential entropy component carries basically healthy skin.

After reordering the channels, we have the lesion region best represented in the first channel. Next, we normalize its values in the range $[0, 1]$ and use the Otsu's thresholding method [18] to segment the skin lesion in this channel. This algorithm assumes two pixel classes, usually background and foreground pixels (specifically in our case, healthy and unhealthy skin pixels), and searches exhaustively for the threshold th that maximizes the inter-class variance $\sigma_b^2(th)$:

$$\sigma_b^2(th) = \omega_1(th)\omega_2(th) \left[\mu_1(th) - \mu_2(th) \right]^2, \quad (3)$$

where, ω_i are the a priori probabilities of the two classes separated by the threshold th, and μ_i are the class means. Given the ICA results, the lesion information can be emphasized (closer to value 1) or de-emphasized (closer to value 0) in this channel, and consequently the thresholded area may correspond to either, the lesion or the background (the only constrain is to maximize σ_b^2). To guarantee that we capture the lesion in the thresholded area, the corners pixels (used in the shading attenuation step, that are known to correspond to healthy skin) are tested to check if they are thresholded as '1's or '0's. If most corner pixels are thresholded as '1's, the thresholded area corresponds to healthy skin, and the logical complement is used to obtain the lesion localization mask. Since the thresholded first re-ordered ICA component now contains the lesion approximately, a morphological opening is performed on this image to better approximate the lesion boundary and eliminate residual artifacts (using a disk of 3 pixels of radius as the structuring element).

C. Lesion Boundary Detection

After obtaining the lesion localization mask (see Section II-B), we determine the lesion boundary more precisely using the Chan-Vese Level-set method for vector-valued images [13]. It assumes that the color image I_i is formed by two regions of approximately constant intensities c_1 and c_2, separated by a curve C. This lesion localization mask is used

as an initialization indicating approximately the region to be segmented. Afterwards, the Level-set method iteratively tries to minimize the energy function $F(c_1, c_2, C)$ in the color image I_i (after shading effects have been attenuated):

$$F(c_1, c_2, C) = \mu\ length(C) + \lambda_1 \int_{inside(C)} \frac{1}{3} \sum_{i=1}^{3} |I_i(x,y) - c_{1,i}|^2\, dxdy + \lambda_2 \int_{outside(C)} \frac{1}{3} \sum_{i=1}^{3} |I_i(x,y) - c_{2,i}|^2\, dxdy,$$

where μ, λ_1 and λ_2 are weighting parameters (we used λ_1=λ_2=1, as suggested by the authors [13], and μ=0.2). Using the Level-set formulation, it is possible to minimize the energy function embedding the curve C, obtaining the zero level set $C(t) = \{(x,y)|\phi(t,x,y) = 0\}$ of a higher dimensional Level-set function $\phi(t,x,y)$. The evolution of $\phi(t,x,y)$ is given by the following motion Partial Differential Equation:

$$\frac{\partial \phi}{\partial t} = \delta_\epsilon(\phi) \left[\begin{array}{l} \mu\ div\left(\frac{\nabla\phi}{|\nabla\phi|}\right) - \\ \frac{1}{3}\sum_{i=1}^{3} \lambda_1 |I_i(x,y) - c_{1,i}|^2 + \\ \frac{1}{3}\sum_{i=1}^{3} \lambda_2 |I_i(x,y) - c_{2,i}|^2 \end{array} \right], \quad (4)$$

where $\delta_\epsilon(\phi)$ is the Dirac delta function, $c_{1,i}$ and $c_{2,i}$ are the averages inside and outside of the curve C in the i-th channel I_i, respectively.

It is possible that the final curve C contains regions beyond the lesion area. So, if the number of regions segmented by the Chan-Vese method is higher than one, local artifacts are eliminated. We compute the area and the perimeter of each segmented region, and cluster these values with K-Means, where K=2. The regions in the cluster with the smaller areas (in average) are eliminated as artifacts and the other regions are kept. The regions kept are hole filled to improve their connectivity, forming the final segmentation mask.

The final post-processing step is a morphological dilation (with a disk of 5 pixels of radius as the structuring element). As already observed [10] [19], the hand labeled lesion ground truth created by specialists tends to be slightly larger than the result of our automatic segmentation, and this dilation operation helps to suppress this difference. Fig. 1 presents images that demonstrate all these steps, from the image shading attenuation until the obtained of lesion segmentation.

III. EXPERIMENTAL RESULTS

In order to evaluate the performance of our proposed segmentation method, we used 141 macroscopic images of pigmented skin lesions from the Dermnet database [20]. In these 141 images, 97 are malignant melanomas images, and 44 are Clark Nevi images (which is a benign lesion

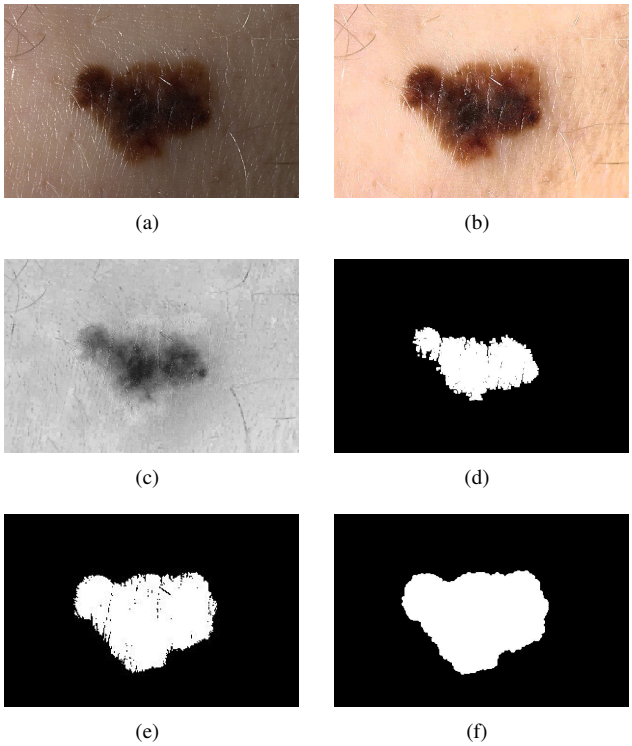

Fig. 1. Illustration of the segmentation process for a pigmented skin lesion image. (a) Original image. (b) Image in (a) after shading attenuation. (c) First re-ordered independent component/channel of image (b). (d) Lesion localization mask. (e) The Level-set segmentation result. (f) Final lesion segmentation, after post-processing image (e).

difficult to diagnose since it contains similar characteristics to melanomas). The segmentation error measure ϵ was chosen because it was also used by the authors of the four state-of-the-art segmentation approaches used in our comparisons [5] [6] [7] [21]:

$$\epsilon = \frac{S \oplus G}{G} \times 100\%, \quad (5)$$

where S is the result of segmentation by the method under test, G is the manual segmentation of the same lesion and $\oplus$ indicates the exclusive-OR, which gives the pixels for which S and G disagree.

We also selected four segmentation methods to compare with the results of our proposed method. In a recent paper, Celebi et al. [10] reviewed several different segmentation approaches for dermoscopy, and indicated two methods among the best performing published approaches: (1) Statistical Region Merging, proposed by Celebi et al. [6]; and (2) Independent Histogram Pursuit, proposed by Gómez et al. [7]. Also recently, Iyatomi et al. [5] proposed a method named "Dermatologist-like", which they claim to obtain segmentation results similar to those obtained by the Celebi et al.[6]. We also included in our comparisons a method recently proposed by Cavalcanti et al. [21], designed specifically for macroscopic images.

Analyzing the segmentation results, we observe that the methods proposed by Celebi et al. [6] and Gómez et al. [7] confuse shading and lesion areas in several images. Probably

sinc(*i*) Research Center for Signals, Systems and Computational Intelligence (fich.unl.edu.ar/sinc)
P. Cavalcanti, J. Scharcanski, L. Di Persia & D. H. Milone; "An ICA-Based Method for the Segmentation of Pigmented Skin Lesions in Macroscopic Images"
33rd Annual International IEEE EMBS Conference (EMBC 2011), pp. 5993-5996, set, 2011.

because these methods have been proposed for dermoscopy images, which are not affected by shading. Also, we generated segmentation results for the 141 images with the three methods mentioned above, using our shading attenuation method as a pre-processing step. The segmentation error averages are presented in Table I, as well as the percentages of the images in the database that generated segmentation errors lower than 5%, 10%, 20%, 30%, 40% and higher than 100%[2], respectively. As it can be seen, our proposed method achieved the best results in all tests in comparison with skin lesion segmentation approaches representative of the state-of-the-art.

TABLE I

COMPARISON OF THE OBTAINED SEGMENTATION ERRORS (IN AVERAGE).

Approach	ϵ in average	ϵ in average w/ Sh. Att.
Celebi et al. [6]	64.80%	42.93%
Gómez et al. [7]	245.70%	123.65%
Iyatomi et al. [5]	29.34%	21.64%
Cavalcanti et al. [21]	25.91%	-
Proposed method	**16.55%**	-

TABLE II

SEGMENTATION ERRORS IN TERMS OF ERROR PERCENTAGES.

Approach	$\epsilon < 10\%$	$\epsilon < 20\%$	$\epsilon < 30\%$	$\epsilon < 40\%$	$\epsilon > 100\%$
Celebi et al. [6]	4.96%	12.77%	20.57%	29.79%	0.71%
Celebi w/ Sh. Att.	2.84%	25.53%	46.81%	58.16%	2.84%
Gómez et al. [7]	14.18%	39.01%	44.68%	46.81%	43.97%
Gómez w/ Sh. Att.	21.28%	58.87%	67.38%	70.92%	20.57%
Iyatomi et al. [5]	14.18%	52.48%	74.47%	83.69%	1.42%
Iyatomi w/ Sh. Att.	19.86%	60.99%	80.85%	90.07%	0.00%
Cavalcanti et al. [21]	22.70%	57.45%	71.63%	79.43%	0.00%
Proposed method	**30.50%**	**75.18%**	**87.94%**	**95.74%**	**0.00%**

IV. CONCLUSIONS AND FUTURE WORK

Several MPSL segmentation methods have been proposed for dermoscopy images, however skin lesion segmentation on macroscopic images have not received much attention. This paper proposes a new method for segmenting pigmented skin lesions on macroscopic images acquired with standard cameras. Our proposed method uses the ICA approach for lesion localization, and a Level-set based segmentation algorithm to obtain more precisely the lesion boundary, which is an important feature to discriminate benign and malignant lesions. In the next stage of this work, we intend to integrate and test our proposed lesion segmentation and boundary detection method in a MPSL pre-screening system, that can be used by non-specialists.

ACKNOWLEDGMENTS

The authors would like to thank CNPq (Brazilian National Council for Scientific and Technological Development), for partially funding this project. This work was also supported by ANPCyT (National Agency for Promotion of Science and Technology, Argentina) under projects PAE 37122 and PAE PICT 00052, and National University of Litoral, under project CAID II R4N14.

[2]The segmentation error is higher than 100% if the segmented area that is not part of the lesion ground truth is larger than the lesion itself.

REFERENCES

[1] J. Mayer, "Systematic review of the diagnostic accuracy of dermatoscopy in detecting malignant melanoma," *The Medical Journal of Australia*, vol. 167, pp. 206–210, 1997.

[2] H. Skvara, L. Teban, M. Fiebiger, M. Binder, and H. Kittler, "Limitations of dermoscopy in the recognition of melanoma," *Arch. Dermatol.*, vol. 141, pp. 155–160, 2005.

[3] C. Massone, E. M. T. Wurm, R. Hofmann-Wellenhof, and H. P. Soyer, "Teledermatology: an update." *Semin. Cutan. Med. Surg.*, vol. 27, no. 1, pp. 101–105, Mar 2008.

[4] J. D. Whited, "Teledermatology research review." *Int. J. Dermatol.*, vol. 45, no. 3, pp. 220–229, Mar 2006.

[5] H. Iyatomi, H. Oka, M. Celebi, M. Hashimoto, M. Hagiwara, M. Tanaka, and K. Ogawa, "An improved internet-based melanoma screening system with dermatologist-like tumor area extraction algorithm," *Computerized Medical Imaging and Graphics*, vol. 32, no. 7, pp. 566 – 579, 2008.

[6] M. E. Celebi, H. A. Kingravi, H. Iyatomi, Y. A. Aslandogan, W. V. Stoecker, R. H. Moss, J. M. Malters, J. M. Grichnik, A. A. Marghoob, H. S. Rabinovitz, and S. W. Menzies, "Border detection in dermoscopy images using statistical region merging." *Skin Res. Technol.*, vol. 14, no. 3, pp. 347–353, Aug 2008.

[7] D. D. Gomez, C. Butakoff, B. K. Ersboll, and W. Stoecker, "Independent histogram pursuit for segmentation of skin lesions," *IEEE Transactions on Biomedical Engineering*, vol. 55, no. 1, pp. 157–161, Jan. 2008.

[8] H. Ganster, A. Pinz, R. Rhrer, E. Wildling, M. Binder, and H. Kittler, "Automated melanoma recognition," *IEEE Transactions on Medical Imaging*, vol. 20, pp. 233–239, 2001.

[9] M. Silveira, J. Nascimento, J. Marques, A. Marcal, T. Mendonca, S. Yamauchi, J. Maeda, and J. Rozeira, "Comparison of segmentation methods for melanoma diagnosis in dermoscopy images," *Selected Topics in Signal Processing, IEEE Journal of*, vol. 3, no. 1, pp. 35 –45, feb. 2009.

[10] M. Celebi, H. Iyatomi, G. Schaefer, and W. V. Stoecker, "Lesion border detection in dermoscopy images," *Computerized Medical Imaging and Graphics*, vol. 33, no. 2, pp. 148 – 153, 2009.

[11] J. Tang, "A multi-direction gvf snake for the segmentation of skin cancer images," *Pattern Recogn.*, vol. 42, pp. 1172–1179, June 2009.

[12] A. Parolin, E. Herzer, and C. R. Jung, "Semi-automated diagnosis of melanoma through the analysis of dermatological images," vol. 0. Los Alamitos, CA, USA: IEEE Computer Society, 2010, pp. 71–78.

[13] T. F. Chan, B. Y. Sandberg, and L. A. Vese, "Active contours without edges for vector-valued images," *Journal of Visual Communication and Image Representation*, vol. 11, no. 2, pp. 130 – 141, 2000.

[14] P. G. Cavalcanti, J. Scharcanski, and C. B. O. Lopes, "Shading attenuation in human skin color images," in *Proc. 6th. International Symposium on Visual Computing (ISVC 2010)*, 2010.

[15] P. G. Cavalcanti and J. Scharcanski, "Automated prescreening of pigmented skin lesions using standard cameras," *to appear in Computerized Medical Imaging and Graphics*, 2011.

[16] A. Hyvärinen, J. Karhunen, and E. Oja, *Independent Component Analysis*. John Wiley & Sons, Inc., 2001.

[17] A. Hyvärinen, "Fast and robust fixed-point algorithms for independent component analysis," *IEEE Transactions on Neural Networks*, vol. 10, no. 3, pp. 626–634, 1999.

[18] N. Otsu, "A threshold selection method from gray-level histograms," *IEEE Transactions on Systems, Man and Cybernetics*, vol. 9, no. 1, pp. 62–66, January 1979.

[19] R. Garnavi, M. Aldeen, M. E. Celebi, G. Varigos, and S. Finch, "Border detection in dermoscopy images using hybrid thresholding on optimized color channels," *Computerized Medical Imaging and Graphics*, vol. 35, no. 2, pp. 105 – 115, 2011, advances in Skin Cancer Image Analysis.

[20] Dermnet skin disease image atlas. [Online]. Available: http://www.dermnet.com

[21] P. G. Cavalcanti, Y. Yari, and J. Scharcanski, "Pigmented skin lesion segmentation on macroscopic images," in *Proc. 25th IEEE Int.Conf. on Image and Vision Computing New Zealand*, 2010.